

Time of flight measurements on ion-velocity distribution and anisotropy of ion temperatures in laser plasmas

Andrea Thum-Jaeger, Binoy K. Sinha,* and Klaus P. Rohr

Fachbereich Physik, Universität Kaiserslautern, D-67663 Kaiserslautern, Germany

(Received 21 December 1999; revised manuscript received 11 September 2000; published 21 December 2000)

Using a 200-mJ, 5-ns, Nd:YAG laser (where YAG denotes yttrium aluminum garnet), time of flight spectra for ions produced from slab targets of carbon, aluminum, nickel, and tantalum were obtained at a laser intensity of approximately $5 \times 10^{10} \text{ W/cm}^2$. The velocity distribution function of ions of each ionization state, at several angles, in the plane of incidence, was investigated and was observed to depart significantly from the Maxwell-Boltzmann distribution function. Kinetic temperatures of ions of each ionization state were estimated separately at various angles in the plane of incidence and were observed to show a highly anisotropic property leading one to conclude that the equipartition of energy between the plasma electrons and ions has not taken place. The results are discussed and the relevant conclusions are presented.

DOI: 10.1103/PhysRevE.63.016405

PACS number(s): 79.20.Ds, 52.50.Jm, 52.20.Hv

I. INTRODUCTION

Laser-produced plasma has drawn the attention of many workers in various fields. Among them are laser fusion at very high laser intensities of 10^{16} – 10^{18} W/cm^2 , laser plasma, and wave-wave interaction at slightly lower intensities varying from 10^{12} to even 10^{18} W/cm^2 . In the fields of material preparation, fabrication of thin films of high- T_c superconductors, oxides, semiconductors, and diamondlike carbon, one often uses laser intensities varying from 10^9 to 10^{12} W/cm^2 . In these investigations, lasers with pulse durations varying from a few femtoseconds to a few nanoseconds have been used. Therefore, one usually has to pay considerable attention to the equilibrium state of the plasma, the energy equipartition between electrons and ions, and the velocity distribution functions for the electrons as well as the ions having different ionization states. These are the basic requirements before one goes into the experimental or theoretical studies of various aspects of the problem.

In various investigations, a Maxwellian or a near-Maxwellian velocity distribution for particles has often been assumed. However, as early as 1988, results were being reported on the nonequilibrium conditions produced in plasma by high-intensity lasers [1]. Recently, Schnürer *et al.* [2], in their experiments on the energy distribution of hot electrons produced by the interaction of short-pulse (0.7 ps–1.05 μm wavelength) and high-intensity ($5 \times 10^{17} \text{ W/cm}^2$) laser beams with solid targets, reported that the electron distribution deviates “significantly from a Maxwell-Boltzmann shape with a single electron temperature parameter.” With recent interest in the deposition of semiconducting and high- T_c superconducting thin films from bulk targets [3–20] and in the analysis of the experimental results obtained so far, one needs to investigate the velocity distribution of the particles. In particular, one needs to know the velocity distribution of the ions of different ionization states, in addition to the en-

ergy equipartition between the electrons and ions and the state of equilibrium for the plasma so produced. Singh and Narayan [3], in this context, have reported that the velocity distribution of the plasma ions is “much broader” than for those having an ideal Maxwellian distribution. Their observation is in agreement with the reported works of earlier investigators [21–23].

With reference to the pulsed-laser evaporation (PLE) technique for the formation of thin films from slab targets, it is observed that the laser-deposition process is always forward-directed in nature [17,20,24]. Depending on the laser parameters of energy, density, and pulse width, thickness variations across the film show a strong dependence on the angle between the target normal and the direction along which the ions are collected [17,20,25]. In addition, the directivity is found to be strongly dependent on the target mass [26], which also follows from the theoretical model of Urbassek and Sibold [16]. To explain this, Kelly and co-workers assumed that the velocity distribution is “probably” Maxwellian [13] and introduced the concept of Knudsen layer formation [10,13,20], which was supported by the theoretical works of Sibold and Urbassek [9,15] and Urbassek and Sibold [16]. They assumed a Maxwellian distribution of particles and the formation of a Knudsen layer to explain the angular steepening of the plasma ions emitted from the solid targets.

To explain the angular steepening of the emitted particles, Sibold and Urbassek [9], Kools *et al.* [12], and Sibold and Urbassek [15] introduced the concept of elliptical temperature for the plasma particles emitted from the target. That is, the particles followed a Maxwell-Boltzmann velocity distribution with two temperatures, one the transversal temperature T_{xy} in the plane of incidence of the laser beam containing the normal to the target (x - y plane), and the other the longitudinal temperature T_z in a direction perpendicular to the plane of incidence. In the present work, we investigated the particle distribution functions for the elements carbon, aluminum, nickel, and tantalum. We have determined the time of flight spectra of the ions of each ionization state and observed their kinetic temperatures for different angles in the plane of incidence. From the experimental results and their

*Present address: Laser and Plasma Technology Division, Bhabha Atomic Research Center, Mumbai-400 085, India.

TABLE I. Energy equipartition time between electrons and ions for $T_e = 30$ eV and $N_i = 10^{18}$, 10^{19} , and 10^{20} ions/cm³.

| Target | Mass number | Average charge \bar{Z} | Equipartition | | |
|----------|-------------|--------------------------|---------------------------------|---|---------------------------|
| | | | $n_i = 10^{18} \text{ cm}^{-3}$ | Time for $T_e = (30 \text{ eV})$ (ns) 10^{19} cm^{-3} | 10^{20} cm^{-3} |
| Carbon | 12 | 2.3 | 11.57 | 1.16 | 0.12 |
| Aluminum | 27 | 2.6 | 20.37 | 2.04 | 0.20 |
| Nickel | 59 | 1.9 | 83.35 | 8.33 | 0.83 |
| Tantalum | 181 | 1.35 | 507.72 | 50.72 | 5.07 |

analysis, it was determined that the particle distribution function departed significantly from a Maxwellian and that the ion temperatures of the expanding plasma were highly anisotropic, leading to the conclusion that the energy equipartition between electrons and ions had not taken place.

II. THEORETICAL CONSIDERATIONS

As we are primarily concerned with the state of the ion velocity distribution function and the concept of elliptical temperatures, it is useful to examine some basic characteristics of the transient plasma with which we are concerned. First, we consider the state of local thermodynamic equilibrium (LTE) in the plasma. Based on the reported works of Mann and Rohr [11] and those of Sinha *et al.* [27] and Sakabe *et al.* [28], at a laser intensity in the vicinity of 10^{11} W/cm^2 , a time- and space-integrated electron temperature of about 30 eV has been estimated and a density of 10^{18} – 10^{20} particles/cm³ has been assumed. If n_e is the electron density of the plasma, then, for the validity of LTE, the following relation, given by Griem [29], has to be satisfied:

$$n_e \geq 9 \times 10^{17} \left(\frac{E_2^{z-1}}{E_H} \right)^3 \left(\frac{kT_e}{E_H} \right)^{1/2} \text{ cm}^{-3}, \quad (1)$$

where E_H is the ionization energy of hydrogen, E_2^{z-1} is the energy level of the second excited state (next to ground level), $Z = 1, 2$, and 3 for neutral, singly, and doubly ionized ions, etc., k is the Boltzmann constant, and T_e is the electron temperature.

Though we have experimentally determined the average ionization state of the plasma in various directions [30], for estimating the requirement of n_e as given by Eq. (1), we use the experimentally determined average ionization state \bar{Z} in a direction perpendicular to the target surface. At a laser energy of 180 mJ (5-ns pulse width, $5 \times 10^{10} \text{ W/cm}^2$ laser intensity), the values for \bar{Z} , in the stated direction, for carbon, aluminum, nickel, and tantalum have been found to be 2.3, 2.6, 1.9, and 1.35, respectively. Based on the experimentally determined values for \bar{Z} , suitable values for E_2^{z-1} have been taken. The inequality relation as given by Eq. (1) for an aluminum plasma at $T_e = 30$ eV and for the validity of LTE works out to be such that

$$n_e \geq (4.3 \times 10^{16}) \text{ cm}^{-3}. \quad (2)$$

Similar figures are obtained for the plasmas produced from carbon, nickel, and tantalum targets as well. Since the plasma has a density varying from 10^{18} to 10^{20} or even 10^{21} cm^{-3} , depending upon the time, the inequalities given by Eqs. (1) and (2) are fully satisfied. Therefore, we are justified in considering the plasmas so produced as having complete LTE.

Second, one has to consider the state of the energy equipartition between the electrons and the ions for the plasma under consideration, as the laser energy is transferred to the electrons first and, then, to the ions through collisions. The electron-ion equilibration or energy equipartition time is given by Spitzer [31] as

$$t_{\text{eq}} = \frac{(0.375)m_e m_i k^{(3/2)}}{(2\pi)^{1/2} n_i Z_e^2 Z_i^2 e^4 \ln \Lambda} \left(\frac{T_e}{m_e} + \frac{T_i}{m_i} \right)^{3/2}, \quad (3)$$

where m_e, m_i denote the masses of electrons and ions in c.g.s. units; k is the Boltzmann constant in erg K^{-1} ; Z_e, Z_i are the charge numbers of electrons and ions; T_e, T_i are the electron and ion temperatures in K; e is the electronic charge in electrostatic units Coulombs; and $\ln \Lambda$ denotes a function that, for wide ranges of plasma parameters, is of order of magnitude 10 [31]. If A_i is the mass number of the ions and if $T_e \approx T_i$ and $m_i \gg m_e$, then the term $T_e/m_e \gg T_i/m_i$. Hence, Eq. (3) can be, after putting in the appropriate numerical values, simplified to

$$t_{\text{eq}} = 24.9 \left(\frac{A_i}{n_i Z_i^2} T_e^{3/2} \right). \quad (4)$$

Using Eq. (4), the energy equipartition times between electrons and ions have been evaluated and they are displayed in Table I. It is observed that as the mass number of the target element increases, the equilibration time also increases because of the factor A_i in the numerator. At an ion density of 10^{18} cm^{-3} and an electron temperature of 30 eV, the times for carbon, aluminum, nickel, and tantalum are given by the values 11.6, 20.4, 83.4, and 507 ns, respectively. That is to say, for a 5-ns pulse width laser, the plasma particles do not have sufficient time to equilibrate during the period of heating by the laser beam, although this requirement is very much relaxed at the higher ion densities of 10^{19} and 10^{20} cm^{-3} . As the electron temperature T_e of the plasma from slab targets varies as t^{-2} and r^{-2} approximately with respect to time (t) and space (r) as analytically deduced and

reported by Rumsby and Paul [32], conditions for the equipartition of energy between electrons and ions are not fully satisfied. Since the equipartition times are short, it is evident from Table I that electrons equilibrate with ions only in a short region of the plasma where the density is relatively high and, more favorably, for low mass number elements such as carbon and aluminum.

To estimate the ion temperature from the time of flight spectra of ions in laser-produced plasma experiments, we proceed as follows. Let the ions follow the Maxwell-Boltzmann distribution for velocities and let the distribution be given by

$$f(u) = I_0 \exp \left[-\frac{1}{2} \frac{m_i (u - u_0)^2}{k T_i} \right], \quad (5)$$

where I_0 denotes an arbitrary constant, u is the ion velocity, u_0 is the ion velocity corresponding to the peak of the distribution function $f(u)$, T_i is the ion temperature, and m_i is the ion mass.

Let R be the radial distance to the ion collector from the target surface. If t is the time for ions to reach the collector from the target surface and $u = (R/t)$ and $u_0 = R/t_0$, where t_0 is the time at which the peak of the time of flight spectra appears, then converting Eq. (5) from the velocity variable u to time variable t , we have

$$f(t) = I_0 \exp \left[-\frac{1}{2} \frac{m_i}{k T_i} R^2 \left(\frac{1}{t} - \frac{1}{t_0} \right)^2 \right]. \quad (6)$$

Let $\Delta t^- = |(t^- - t_0)|$ be the half temporal width at half maximum of the function $f(t)$ approaching towards the higher velocity of the particles. Let $\Delta t^+ = |(t^+ - t_0)|$ be the half temporal width at half maximum of the function $f(t)$ approaching the lower velocity of the particles. The symbols t^- and t^+ denote times to the left and right of t_0 , where the values of the function $f(t)$ are half the peak value at $t = t_0$. If the distribution function is truly Maxwellian, the function $f(t)$ will be symmetrical and, in that case,

$$\Delta t^- = \Delta t^+ \quad \text{or} \quad \frac{\Delta t^+}{\Delta t^-} = 1. \quad (7)$$

The degree of departure of the ratio $(\Delta t^+/\Delta t^-)$ from unity will be a measure of departure of the distribution function $f(t)$ from a Maxwellian one. For times close to t_0 , $t_0 \gg \Delta t^-$ or Δt^+ and Eq. (6) can be used to estimate the ion temperature, such that

$$T_i = \frac{1}{2k \ln 2} \frac{m R^2}{t_0^4} (\Delta t^-)^2 \quad (8)$$

or

$$T_i = \frac{1}{2k \ln 2} m u_0^2 \left(\frac{\Delta t^-}{t_0} \right)^2 \quad (8a)$$

or

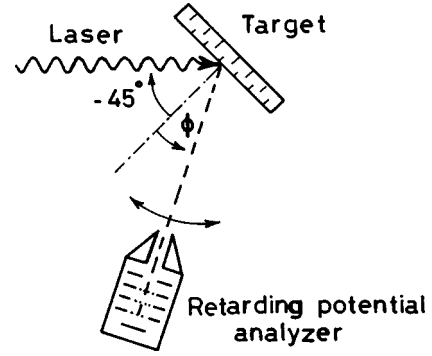


FIG. 1. A schematic diagram of the experimental setup.

$$T_i = \frac{1}{2k \ln 2} m u_0^2 \left(\frac{\Delta t^+}{t_0} \right)^2. \quad (8b)$$

A similar technique to estimate the ion temperature from time of flight spectra has been used by Stritzker *et al.* [23]. We have used Eq. (8a) to estimate the ion temperature at times $t \leq t_0$ as we have found from the time of flight spectra that the distribution shows a significant departure from Maxwellian for values of $t \gg t_0$. The possible reasons for departure of the function $f(t)$ from truly Maxwellian will be reported in Sec. IV.

III. THE EXPERIMENTAL ARRANGEMENT

A schematic representation of the experimental arrangement is given in Fig. 1. The plasma is created by a Nd-YAG (yttrium aluminum garnet) Q -switch pulse ($\tau = 5$ ns, $\lambda = 1.06 \mu\text{m}$) in the TEM₀₀ mode of variable energy, incident at a fixed angle of -45° onto flat, rotating targets inside a vacuum chamber. The investigated materials are C ($M = 12$, $A = 6$), Al ($M = 27$, $A = 13$), Ti ($M = 48$, $A = 22$), Ni ($M = 59$, $A = 28$), Mo ($M = 96$, $A = 42$), and Ta ($M = 181$, $A = 73$). The laser energy ranges from about 20 to 180 mJ and is focused to intensities from about 10^{10} to 10^{11} W/cm^2 . The freely expanding ions of the plasma are measured in an angular range between about $\phi = -17.5^\circ$ to 60° relative to the target normal by moving the detector within the plane of incidence at a distance of 37.5 cm from the target. Analysis of the ion velocity distribution and charge is performed by means of a time-of-flight-retarding potential detector whose transmission function has been controlled carefully [11]. Some additional effort has been necessary to increase the reliability of the results and to be able to obtain absolute values of the ion fluxes. These include the following: (i) keeping the $n \times 1$ product [(residual gas density) \times (plasma flight distance)] at least an order of magnitude below the critical value of $5 \times 10^{13} \text{ cm}^{-2}$, deduced from cross-section data of Schwarz *et al.* [33]; (ii) removing surface contaminations from the target by using defocused prepulses; (iii) minimizing the changes of ion emission distribution due to cratering by rotating the target after a certain number of shots, empirically determined to be below 10.

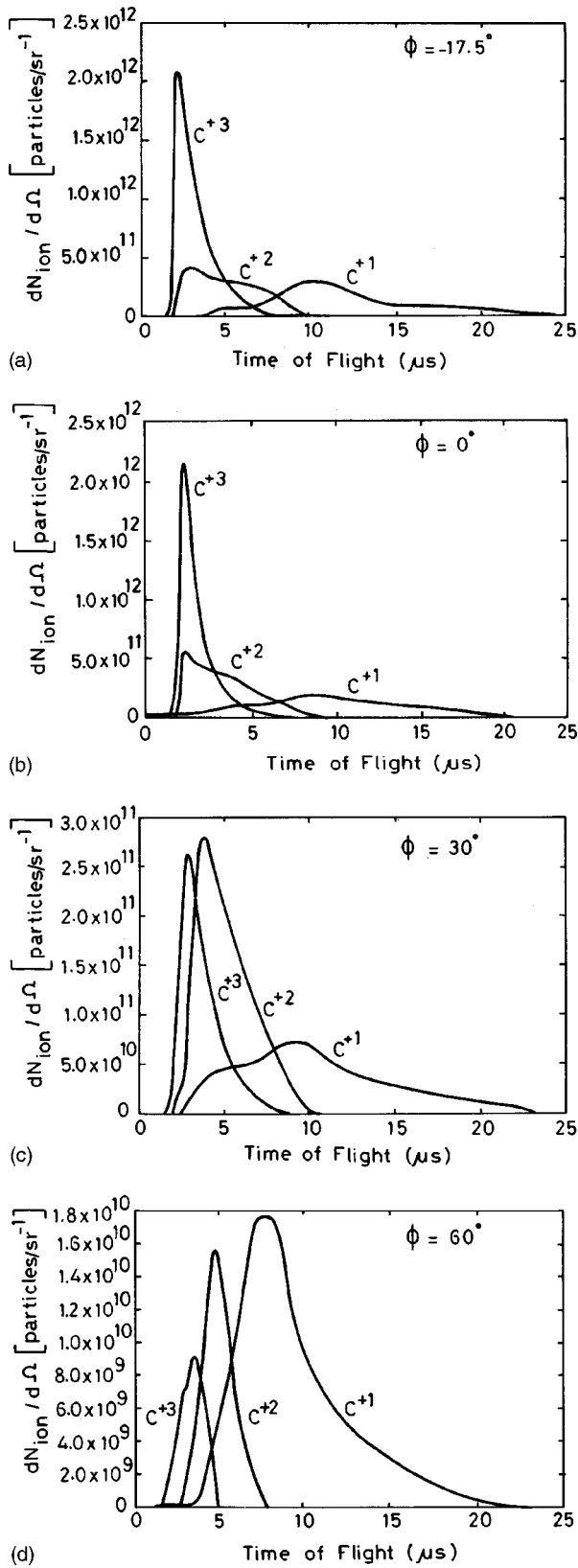


FIG. 2. Time of flight spectra of carbon ions emitted per unit time per unit solid angle as a function of flight time at angles of emission $\Phi = -17.5^\circ$ (a), 0° (b), 30° (c), and 60° (d). Singly, doubly, and triply ionized states are shown by the symbols C^{+1} , C^{+2} , and C^{+3} , respectively.

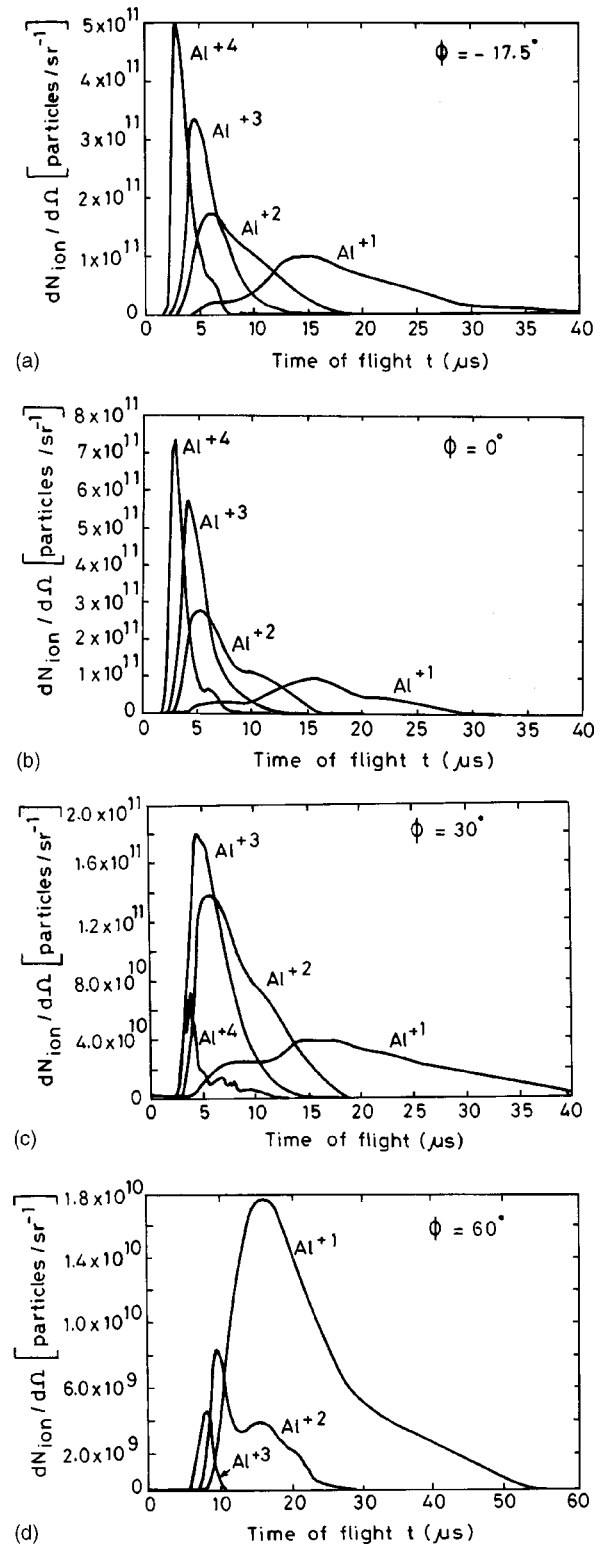


FIG. 3. Time of flight spectra of aluminum ions emitted per unit time per unit solid angle as a function of flight time at angles of emission $\Phi = -17.5^\circ$ (a), 0° (b), 30° (c), and 60° (d). Singly, doubly, triply, and quadruply times ionized stages are shown by the symbols Al^{+1} , Al^{+2} , Al^{+3} , and Al^{+4} , respectively.

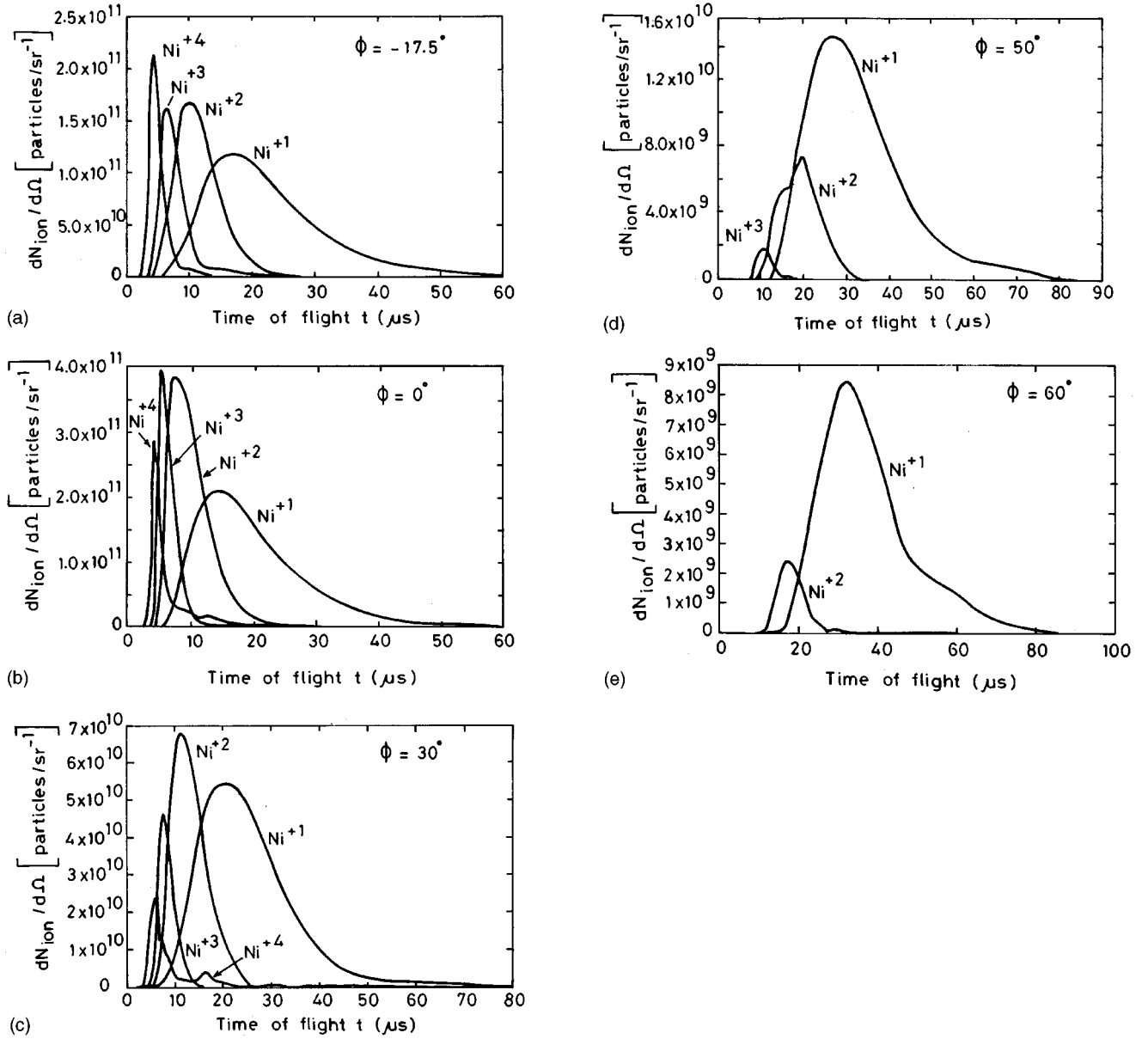


FIG. 4. Time of flight spectra of nickel ions emitted per unit time per unit solid angle as a function of flight time at angles of emission $\Phi = -17.5^\circ$ (a), 0° (b), 30° (c), 50° (d), and 60° (e). Different ionization states are indicated.

The signal of the detector is stored at a digitizing rate of 100 MHz. By multiscaling, an effective resolution of about 10 bits is obtained. The total uncertainty of the absolute flux of the evaluated differential ion spectra is estimated to range from 5% for the low energetic part to about 30% for the highest charges and kinetic energies of the ions. The increase of the uncertainty with the increase in the degree of ionization and the kinetic energy of the ions is inherent in the analyzing procedure of the TOF-retarding potential method. The detailed experimental procedures are well described in the works of Mann and Rohr [11] and Demtröder and Jantz [34]. The laser energy is determined by a calorimeter in absolute units (Type RJP700 of Laser Precision Corporation). It is monitored continuously and has a shot-to-shot variation within 3%. The laser pulse is essentially TEM₀₀ (spatially

controlled by a CCD camera). The beam has a divergence of about 0.3 mrad with a full width at half maximum pulse width value of 5 ns.

IV. RESULTS AND DISCUSSION

In Figs. 2–5, we have displayed the time of flight measurements for the absolute number of ions emitted per unit solid angle as a function of time of flight for each available ionization state for the elements carbon, aluminum, nickel, and tantalum at various angles of particle emission while using a constant laser energy of 180 mJ. The angle of emission Φ was defined as an angle between the line of observation and the normal to the target plane on the plane of incidence of the laser beam. Though the angle was varied

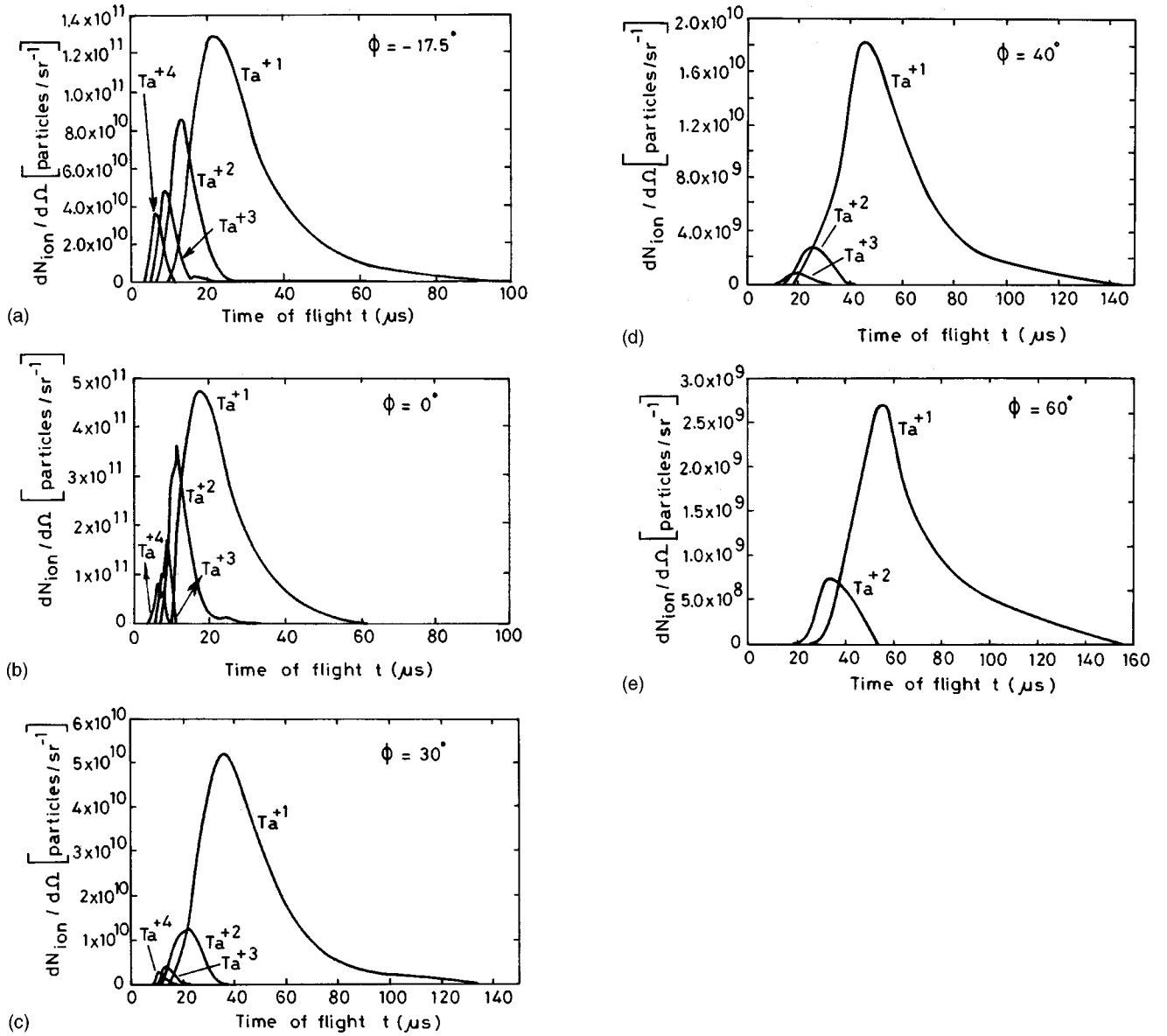


FIG. 5. Time of flight spectra of tantalum ions emitted per unit time per unit solid angle as a function of flight time at angles of emission $\Phi = -17.5^\circ$ (a), 0° (b), 30° (c), 40° (d), and 60° (e). The different ionization states are indicated.

between -17.5° and 60° at an interval of 5° , only selected angles are displayed in Figs. 2–5 as the data obtained are voluminous. In Figs. 2(a)–2(d) we have displayed the results for singly, doubly, and triply ionized carbon atoms. Note that at angles $\Phi = -17.5^\circ$ and 0° , C^{+3} ions ($\approx 2 \times 10^{12}$ ions) numerically dominate over C^{+2} and C^{+1} ions by a factor of approximately 10. As the angle of observation moves to 30° and 60° , the total number of ions emitted is reduced by an order of magnitude. At $\Phi = 30^\circ$, the concentration of C^{+3} and C^{+2} ions becomes nearly equal, but is still nearly ten times more than that of C^{+1} ions. At $\Phi = 60^\circ$, the total number of ions is very much reduced ($\approx 10^{10}$ ions) but the relative concentration of ions is in reverse order with reference to those at $\Phi = -17.5^\circ$ and 0° . That is to say, now the concentration of C^{+1} ions (1.7×10^{10}) is higher than that of C^{+2} (1.5×10^{10}) and C^{+2} ions are much more abundant than those of C^{+3} ($\approx 10^9$). From a check of the symmetry of the

time of flight spectra, it is obvious that there is a significant departure from the Maxwell-Boltzmann distribution function. The asymmetry of the distribution function is numerically represented in Table II, which will be discussed subsequently.

Similar results are displayed for aluminum [Figs. 3(a)–3(d)], nickel [Figs. 4(a)–4(e)], and for tantalum [Figs. 5(a)–5(e)]. It is observed that the maximum number of particles is emitted along a direction normal to the target surface and, then, decreases sharply as one goes away from the normal. For elements of comparatively low mass numbers such as carbon and aluminum, the ions of the highest ionization state dominate in the direction of maximum emission, and then their concentration falls sharply as one goes away from the normal. This trend is diluted as we arrive at nickel. In this case, ions of ionization state 3 dominate over those of the ionization state 4. For tantalum, the trend is completely re-

TABLE II. Asymmetry of the distribution function and the estimate of the temperature for some typical ions.

| Ions | Angle of emission (deg) | Mass number A_i | Asymmetry factor $f = \frac{\Delta t^+}{\Delta t^-}$ | Ion temperature in eV error $\pm 20\%$ |
|------------|-------------------------|-------------------|--|--|
| C^{+3} | -17.5 | 12 | 2.36 | 88.2 |
| C^{+1} | -17.5 | 12 | 1.11 | 6.2 |
| C^{+3} | 0.0 | 12 | 1.12 | 102.2 |
| C^{+1} | 0.0 | 12 | 0.82 | 25.8 |
| C^{+3} | 60 | 12 | 0.86 | 57.6 |
| C^{+2} | 60 | 12 | 0.99 | 17.2 |
| C^{+1} | 60 | 12 | 1.32 | 9.2 |
| Al^{+4} | -17.5 | 27 | 1.67 | 145.0 |
| Al^{+3} | -17.5 | 27 | 3.33 | 28.0 |
| Al^{+2} | -17.5 | 27 | 2.22 | 17.6 |
| Al^{+1} | -17.5 | 27 | 1.94 | 8.4 |
| Al^{+3} | 40.0 | 27 | 1.58 | 63.0 |
| Al^{+2} | 40.0 | 27 | 2.90 | 22.4 |
| Al^{+1} | 40.0 | 27 | 1.45 | 33.4 |
| N_i^{+4} | 0.0 | 59 | 0.99 | 132.2 |
| N_i^{+3} | 0.0 | 59 | 1.24 | 108.8 |
| N_i^{+2} | 0.0 | 59 | 1.59 | 82.0 |
| N_i^{+1} | 0.0 | 59 | 1.60 | 38.6 |
| Ta^{+3} | 15.0 | 181 | 1.38 | 65.6 |
| Ta^{+2} | 15.0 | 181 | 1.60 | 54.6 |
| Ta^{+1} | 15.0 | 181 | 1.58 | 36.8 |

versed. Now, along the direction of the normal to the target surface, ions of ionization state 1 are much more in abundance than those of the state 4.

In Figs. 6–9, we have displayed the variation of kinetic temperatures of ions of different ionization stages for carbon

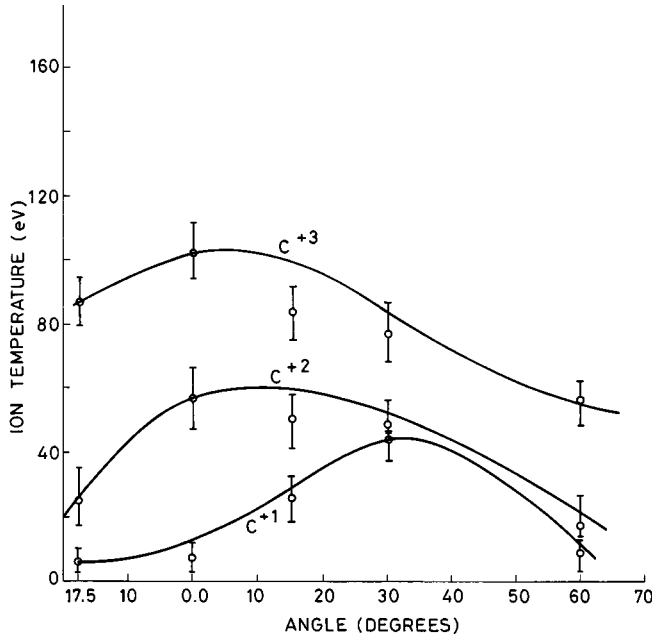


FIG. 6. Angular variation of the temperature of C^{+1} , C^{+2} , and C^{+3} ions.

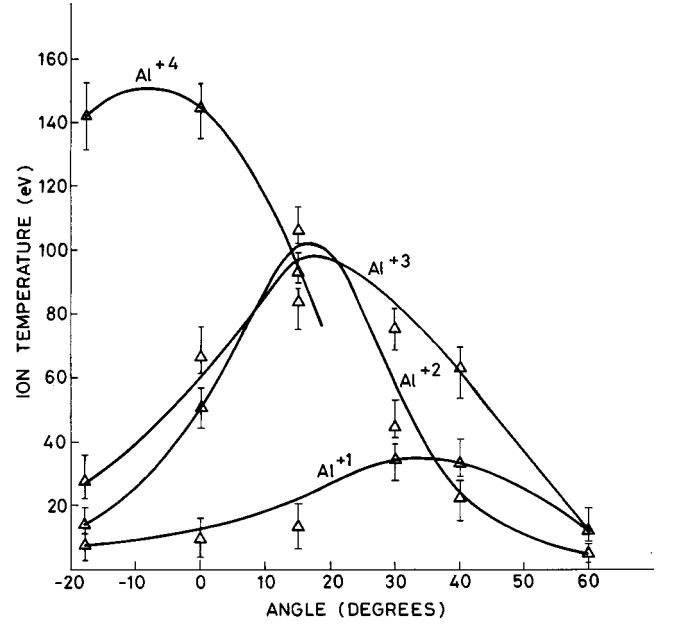


FIG. 7. Angular variation of the temperature of Al^{+1} , Al^{+2} , Al^{+3} , and Al^{+4} ions.

(Fig. 6), aluminum (Fig. 7), nickel (Fig. 8), and tantalum (Fig. 9) as a function of the angles of emission for the same laser energy of 180 mJ. In all the figures we observe that the higher the ionization state, the greater the kinetic temperature, which is probably because of enhanced absorption of laser light in the high-Z region of the plasma. Thus, ions of ionization state 1 show the lowest values for the temperature at any given angle and those of states 3 and 4 show higher values. The variation of the ion temperatures is quite aniso-

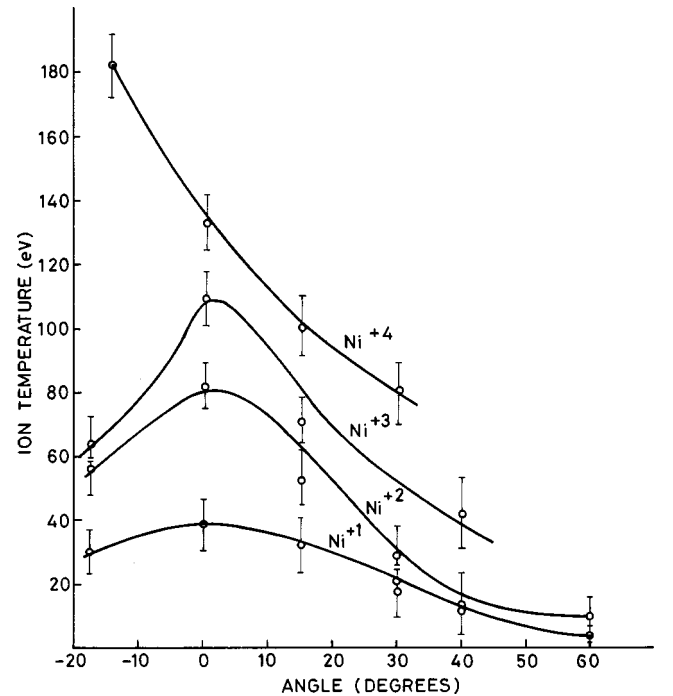


FIG. 8. Angular variation of the temperature of N_i^{+1} , N_i^{+2} , N_i^{+3} , and N_i^{+4} ions.

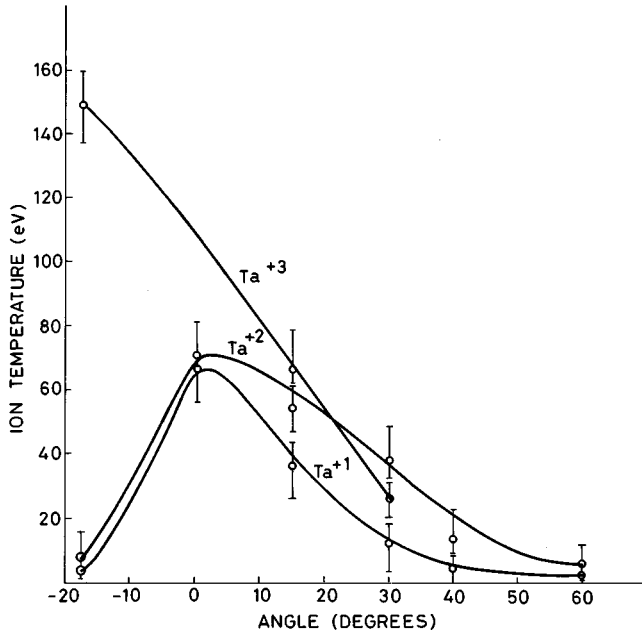


FIG. 9. Angular variation of the temperature of T_a^{+1} , T_a^{+2} , T_a^{+3} , and T_a^{+4} ions.

tropic and the angles corresponding to the peaks of temperature variation are different for different ionization states and mass numbers. In other words, one can say that the equipartition of energy between electrons and ions has not taken place. Were it so, the temperature variation would have been isotropic.

After the plasma is created by a 5-ns laser pulse, it expands radially outwards from the target into vacuum with no sources or sinks for energy, density, or states of ionization. The front boundary of the plasma expands freely into vacuum at a constant velocity and the whole of the plasma expands uniformly preserving a normalized density profile (shape normalized to peak density and expansion radius) [32,35]. The laser-produced plasma under consideration is highly collisional with all collision times much shorter than the laser pulse. Using the basic formulation of plasma physics, a typical electron-ion collision time for $T_e = 30$ eV and $n_i = 10^{18} \text{ cm}^{-3}$ is approximately 10^{-2} ns, which is much smaller than the laser pulse width. As in the case of the adiabatic expansion of the laser plasma, the electron temperature and density approximately show temporal variation as t^{-2} and t^{-3} , respectively. Particle collision time, which varies as $(T_e^{3/2}/n_e)$, would remain nearly constant as the expansion proceeds [32].

During the adiabatic expansion of the plasma, three recombination processes come into play [18,32,36]: (i) radiative, (ii) three-body, and (iii) dielectronic. After the laser action has terminated, the ion composition of the plasma mainly changes due to the effect of the three-body recombination, which dominates over the radiative and dielectronic ones due to a large drop in the electron temperature as the plasma expands into vacuum. Three-body recombination has a strong influence on the charge composition throughout the entire duration of the plasma expansion, right up to the time when it enters the detectors [37]. The ions located at the front

of the expanding plasma acquire the largest energy during the hydrodynamic acceleration and, thereby, the interaction time for recombination is very much reduced. As a result, their charge composition is considerably less influenced by recombination, and the average charge of the ions in the high-energy part of the spectrum roughly corresponds to that in the heating phase. But the ions located in the inner plasma layers are accelerated much less during the hydrodynamic expansion and remain much longer in the denser state, which results in being subjected to strong recombination [37]. Therefore, in estimating the ion temperature from Eqs. (8a) or (8b), we have preferred Eq. (8a), in which the value for Δt^- is less influenced than the value for Δt^+ due to recombination.

It is a bit hazardous to estimate to what extent the recombination processes broaden the distribution profile due to a lack of sufficient recombination and ionization data. But two important observations may be made about the ion velocity distribution. First, the distribution function is no longer Maxwellian and is not symmetric. Second, time of flight spectra of ions from high mass number elements such as nickel and tantalum are smoother and show less departure from Maxwellian than those of ions from low mass number such as carbon and aluminum. In Table II, we have displayed the asymmetry of the distribution function for some representative ions and some of the angles of emission. The asymmetry of the distribution function is defined by the factor $f = (\Delta t^+/\Delta t^-)$ [see Eq. (7)]. The departure from unity is a measure of departure from a Maxwellian distribution.

One can see from the table that, for higher mass number elements such as N_i and T_a , the departure from a Maxwellian profile is less than 60%, but for low mass ions such as carbon and aluminum, the variation ranges from a few percent to the order of 200% or more. In other words, the profiles of the time of flight spectra for high mass number ions such as nickel and tantalum seem to be closer to Maxwellian than those for low mass number ions such as carbon and aluminum. In the expanding plasma, the ion composition is chiefly influenced by the three-body recombination, which varies as Z^3/T_e [37,38]. One of the possible reasons for the above results is the average ionization state of the plasma. From Table I, we note that the average ionization states of carbon, aluminum, nickel, and tantalum, as experimentally determined, are given by the values 2.3, 2.6, 1.9, and 1.35, respectively. As a result, due to the Z^3 factor, nickel and tantalum ions are subjected less to three-body recombination than those of carbon and aluminum. As a result, there is somewhat less of a departure from the ideal profile.

Since there is little available experimental information about the distribution function of particles emitted from laser-produced plasmas, we consider the works of Bykovskii *et al.* [39]. They made a mass-spectrometric investigation of the neutral particles of a plasma produced from targets of carbon, aluminum, cadmium, and lead and studied the distribution function of the neutral particles in the laser-intensity range of $10^7 - 10^{10} \text{ W/cm}^2$. They reported that the distribution functions so obtained are Maxwellian and ascribed their results to the thermal origin of the atom formation. In our experiments, the particle emission is not purely thermal, but

is also electronic [14,39]. The complex processes of plasma physics are involved, giving rise to a departure from a Maxwellian distribution.

It is further seen from the present measurements that around 90% of the ions are emitted approximately along the normal to the target surface. From Figs. 6–9, one can see that these ions generally represent the particles with nearly the highest kinetic temperatures for each ionization state. A detailed investigation for this streaming emission of the ions along the direction normal to the target surface will be reported separately, though some explanation has already been given in earlier work [15,16,20].

V. CONCLUSIONS

On the basis of the results and discussion presented in Sec. IV, it is possible to draw the following conclusions.

(i) About 90% of the plasma ions, under the conditions of the present experiment, are emitted along a direction normal to the target. Moreover, these ions represent the hottest part of the plasma ions and they carry with them the major portion of the plasma thermal energy. Additionally, along this direction the ions of higher ionization state always have higher values of temperature than those for lower ionization states.

(ii) The ion velocity distribution function as determined from time of flight spectra shows a significant departure from the Maxwellian profile. The asymmetry factor “ f ” as defined above approximately gives a measure of departure from the Maxwellian distribution. This factor shows a maximum de-

parture of 60% for ions of high mass numbers such as nickel and tantalum and, in some cases, as great as 200% for ions of low mass numbers such as carbon and aluminum. In general, the ion velocity distribution profiles are smoother and show less departure from a Maxwellian one in the case of ions of higher mass numbers than in the case of those with lower mass numbers. This is true for ions of each ionization state varying from one to four.

(iii) The angular variation of temperature for ions of any ionization state and any mass number, in the plane of incidence, is completely anisotropic and, hence, it is concluded that the equipartition of energy between electrons and ions has not taken place.

(iv) Recombination mechanisms like those of radiative, three-body, and dielectronic processes possibly have an important role in broadening the ion velocity profile during the course of the adiabatic expansion. This problem, we think, is very interesting from theoretical as well as experimental points of view.

ACKNOWLEDGMENTS

This work has been supported by the Deutsche Forschungsgemeinschaft. One of us (B.K.S.) gratefully acknowledges the extraordinary leave granted by the Trombay Committee and the Trombay Scientific Committee of Bhabha Atomic Research Center, Mumbai, India and the Alexander von Humboldt Foundation, Bonn, Germany. The technical assistance of Hans Feurich is acknowledged.

-
- [1] G. Gibson, R. Rosman, T. S. Luk, I. A. McIntyre, A. McPherson, G. Wendim, K. Boyer, and C. K. Rhodes, in *Proceedings of the OSA Topical Meeting on Short Wavelength Coherent Radiation: Generation and Applications, North Falmouth, Cape Cod, MA, September 1988*, pp. 246-250.
 - [2] M. Schnürer, R. Nolte, T. Schlegel, M. P. Kalachnikov, P. V. Nickles, P. Ambrosi, and W. Sandner, *J. Phys. B* (to be published).
 - [3] R. K. Singh and J. Narayan, *Phys. Rev. B* **41**, 8843 (1990).
 - [4] D. Dijkamp, T. Venkatesan, X. D. Wu, S. A. Shaheen, N. Jisrawi, Y. H. Min-lee, W. L. McLean, and M. Croft, *Appl. Phys. Lett.* **51**, 619 (1987).
 - [5] D. K. Fork, J. B. Boyce, F. A. Ponce, R. I. Johnson, G. B. Anderson, G. A. N. Connell, C. B. Com, and T. H. Geballe, *Appl. Phys. Lett.* **53**, 337 (1988).
 - [6] C. R. Guarieri, R. A. Roy, K. L. Saenger, S. A. Shivshankar, D. S. Yee, and J. J. Cuomo, *Appl. Phys. Lett.* **53**, 532 (1988).
 - [7] R. K. Singh, O. W. Holland, and J. Narayan, *J. Appl. Phys.* **68**, 233 (1990).
 - [8] R. Kelly, *Nucl. Instrum. Methods Phys. Res. B* **46**, 441 (1990).
 - [9] D. Sibold and H. M. Urbassek, *Phys. Rev. A* **43**, 6722 (1991).
 - [10] R. Kelly and B. Braren, *Appl. Phys. B: Photophys. Laser Chem.* **53**, 160 (1991).
 - [11] K. Mann and K. Rohr, *Laser Part. Beams* **10**, 435 (1992).
 - [12] J. C. S. Kools, T. S. Baller, S. T. DeZwart, and J. Dieleman, *J. Appl. Phys.* **71**, 4547 (1992).
 - [13] Roger Kelly, *Phys. Rev. A* **46**, 860 (1992).
 - [14] R. Kelly, A. Miotello, B. Braren, A. Gupta, and K. Casey, *Nucl. Instrum. Methods Phys. Res. B* **65**, 187 (1992).
 - [15] D. Sibold and H. M. Urbassek, *J. Appl. Phys.* **73**, 8544 (1993).
 - [16] H. M. Urbassek and D. Sibold, *Phys. Rev. Lett.* **70**, 1886 (1993).
 - [17] A. Thum, A. Rupp, and K. Rohr, *J. Phys. D* **27**, 1791 (1994).
 - [18] G. Granse, S. Völlmar, A. Lenk, A. Rupp, and K. Rohr, *Appl. Surf. Sci.* **96–98**, 97 (1996).
 - [19] P. Schreiner and H. M. Urbassek, *J. Phys. D* **30**, 185 (1997).
 - [20] R. Kelly and R. W. Dreyfus, *Nucl. Instrum. Methods Phys. Res. B* **32**, 341 (1988).
 - [21] T. Ventatesan, X. D. Wu, A. Inam, Y. Jeon, M. Croft, E. W. Chase, C. C. Chang, J. B. Watchman, R. W. Odom, F. R. di Brozolo, and C. A. Magel, *Appl. Phys. Lett.* **53**, 1431 (1988).
 - [22] T. Nakayama, M. Okogawa, and N. Itoh, *Nucl. Instrum. Methods Phys. Res. B* **1**, 301 (1984).
 - [23] B. Stritzker, A. Pospieszczyk, and J. A. Tagle, *Phys. Rev. Lett.* **47**, 356 (1981).
 - [24] R. K. Singh, N. Biunno, and J. Narayan, *Appl. Phys. Lett.* **53**, 1013 (1988).
 - [25] R. A. Neifeld, S. Gunapala, C. Liang, S. A. Shaheen, M. Croft, S. Price, D. Simmons, and W. T. Hill, *Appl. Phys. Lett.* **53**, 703 (1988).
 - [26] A. Thum-Jaeger and K. Rohr, *J. Phys. D* **32**, 2827 (1999).

- [27] B. K. Sinha, S. R. Kumbhare, and G. P. Gupta, Phys. Rev. A **41**, 3294 (1990).
- [28] S. K. Sakabe, T. Mochizuki, T. Yabe, K. Mima, and C. Yamanaka, Phys. Rev. A **26**, 2159 (1982).
- [29] H. R. Griem, *Plasma Spectroscopy* (McGraw Hill, New York, 1964), pp. 150–156.
- [30] A. Thum-Jaeger, B. K. Sinha, and K. P. Rohr, Phys. Rev. E **61**, 3063 (2000).
- [31] Lyman Spitzer, *Physics of Fully Ionized Gases*, 2nd ed. (Wiley Interscience, New York, 1962), pp. 131–136.
- [32] T. P. Rumsby and J. W. M. Paul, Plasma Phys. **16**, 247 (1974).
- [33] U. Schwartz, F. Linder, and K. Rohr, J. Phys. B **28**, 839 (1995).
- [34] W. Demtröder and W. Jantz, Plasma Phys. **12**, 691 (1970).
- [35] Ya. B. Zeldovich and Yu. P. Raizer, *Physics of Shock Waves—Temperature Phenomena* (Academic, New York, 1966).
- [36] S. V. Latyshev and I. V. Rudskoi, Sov. J. Plasma Phys. **11**, 669 (1985).
- [37] A. A. Golubev, S. V. Latyshev, and B. Yu. Sharkov, Sov. J. Quantum Electron. **14**, 1242 (1984).
- [38] I. I. Sobelman, L. A. Vainshtein, and E. A. Yukov, *Excitations of Atoms and Broadening of Spectral Lines* (Springer Verlag, Berlin, 1981).
- [39] Yu. A. Bykovskii, S. M. Silnov, E. A. Sotnichenko, and B. A. Sheshtakov, Zh. Eksp. Teor. Fiz. **93**, 500 (1987) [Sov. Phys. JETP **66**, 285 (1987)].